TSINGHUA SCIENCE AND TECHNOLOGY
ISSN 1007-0214 09/18 pp61-66
Volume 10, Number 1, February 2005

Meshless Least-Squares Method for Solving the Steady-State Heat Conduction Equation*

LIU Yan (刘 岩), ZHANG Xiong (张 雄)**, LU Mingwan (陆明万)

School of Aerospace, Tsinghua University, Beijing 100084, China

Abstract: The meshless weighted least-squares (MWLS) method is a pure meshless method that combines the moving least-squares approximation scheme and least-square discretization. Previous studies of the MWLS method for elastostatics and wave propagation problems have shown that the MWLS method possesses several advantages, such as high accuracy, high convergence rate, good stability, and high computational efficiency. In this paper, the MWLS method is extended to heat conduction problems. The MWLS computational parameters are chosen based on a thorough numerical study of 1-dimensional problems. Several 2-dimensional examples show that the MWLS method is much faster than the element free Galerkin method (EFGM), while the accuracy of the MWLS method is close to, or even better than the EFGM. These numerical results demonstrate that the MWLS method has good potential for numerical analyses of heat transfer problems.

Key words: meshless; least-squares; heat conduction; steady-state

Introduction

In the past twenty years, a series of numerical methods called meshless methods (also called meshfree methods) have been developing rapidly. The first meshless method was smoothed particle hydrodynamics developed by Lucy[1] and Gingold and Monaghan[2] in 1977, and then thoroughly studied by Monaghan[3]. After the element free Galerkin method (EFGM) was proposed by Belytschko et al. in 1994[4], meshless methods have drawn more and more attention and have been successfully applied to various problems in solid mechanics, fluid mechanics, heat transfer, and electromagnetic fields[5-7].

Most kinds of meshless methods have been built upon discretization schemes like the Galerkin method, the Petrov-Galerkin method, or the direct collocation method. Generally speaking, meshless methods of the Galerkin and Petrov-Galerkin types need numerical integration, which results in much more computational effort than the finite element method (FEM) in most cases; while the direct collocation meshless method suffers from instabilities.

Like the least-squares finite element method (LSFEM)[8], meshless methods can also be based on least-square schemes. The meshless weighted least-squares (MWLS) method[9] is such a method. Application of MWLS to elastostatics and wave propagation problems has shown that it is accurate, stable, and efficient.

In this paper, the MWLS method is extended to solve heat conduction problems. The basic MWLS formulation for solving steady-state heat conduction problems is developed, and the optimal choice of computational parameters is discussed. Several 2-D examples are presented with the numerical results compared with analytical and EFGM solutions.

Received: 2004-08-10

* Supported by the National Natural Science Foundation of China (No. 10172052)

** To whom correspondence should be addressed.
E-mail: xzhang@tsinghua.edu.cn; Tel: 86-10-62782078-1

1 Moving Least-Squares Approximation

In the moving least-squares (MLS) scheme, the local approximation of the field variable $u(\boldsymbol{x})$ is expressed as

$$u(\boldsymbol{x}) \approx u^h(\boldsymbol{x}, \bar{\boldsymbol{x}}) = \sum_{i=1}^{m} p_i(\bar{\boldsymbol{x}}) a_i(\boldsymbol{x}) = \boldsymbol{p}^{\mathrm{T}}(\bar{\boldsymbol{x}}) \boldsymbol{a}(\boldsymbol{x}) \quad (1)$$

where $p_i(\bar{\boldsymbol{x}})$ is the basis function, generally a complete monomial, m is the number of terms in the basis function, and $a_i(\boldsymbol{x})$ are the coefficients, which are determined by minimizing the following L_2 norm,

$$J = \sum_I w_I(\boldsymbol{x}) \left(u^h(\boldsymbol{x}, \boldsymbol{x}_I) - u(\boldsymbol{x}_I) \right)^2 = \sum_I w_I(\boldsymbol{x}) \left[\boldsymbol{p}^{\mathrm{T}}(\boldsymbol{x}_I) \boldsymbol{a}(\boldsymbol{x}) - u_I \right]^2 \quad (2)$$

where u_I is the value of $u(\boldsymbol{x})$ at node $\boldsymbol{x}_I$, and $w_I(\boldsymbol{x})$ is the weight function that is usually a compactly supported function which is only nonzero in a small neighborhood called the “support domain” of node $\boldsymbol{x}_I$ where it reaches its maximum value. Many kinds of weight functions have been used in meshless methods. The cubic spline function is used in this paper,

$$w(r) = \begin{cases} 2/3 - 4r^2 + 4r^3, & r \le 1/2; \\ 4/3 - 4r + 4r^2 - 4r^3/3, & 1/2 < r \le 1; \\ 0, & r > 1 \end{cases} \quad (3)$$

where r is the normalized radius equal to the ratio of the distance between node I and the evaluation point to the radius of the support domain.

The minimization of the function J is equivalent to

$$\frac{\partial J}{\partial \boldsymbol{a}} = \boldsymbol{A}(\boldsymbol{x}) \boldsymbol{a}(\boldsymbol{x}) - \boldsymbol{B}(\boldsymbol{x}) \boldsymbol{u} = \boldsymbol{0} \quad (4)$$

where the matrices are given by

$$\boldsymbol{A}(\boldsymbol{x}) = \sum_{I=1}^{n} w_I(\boldsymbol{x}) \boldsymbol{p}(\boldsymbol{x}_I) \boldsymbol{p}^{\mathrm{T}}(\boldsymbol{x}_I),$$

$$\boldsymbol{B}_I(\boldsymbol{x}) = w_I(\boldsymbol{x}) \, \boldsymbol{p}(\boldsymbol{x}_I) \quad (5)$$

$$\boldsymbol{u} = \left(u_1, \quad u_2, \quad \cdots, \quad u_n \right)^{\mathrm{T}} \quad (6)$$

Substituting the coefficients $\boldsymbol{a}(\boldsymbol{x})$ from Eq. (4) into Eq. (1), the MLS approximation can be expressed as

$$u^h(\boldsymbol{x}) = \sum_{I=1}^{n} N_I(\boldsymbol{x}) \, u_I \quad (7)$$

where the shape function $N_I(\boldsymbol{x}) = \boldsymbol{p}^{\mathrm{T}}(\boldsymbol{x}) \boldsymbol{A}^{-1}(\boldsymbol{x}) \boldsymbol{B}_I(\boldsymbol{x})$.

2 Basic Equations for Heat Conduction Problems and the Least-Squares Discretization

The steady-state temperature distribution in domain Ω is governed by

$$k\nabla^2 u(\boldsymbol{x}) + \rho Q = 0, \qquad \boldsymbol{x} \in \Omega \quad (8)$$

with the boundary conditions:

$$u = \bar{u}, \qquad \boldsymbol{x} \in \Gamma_1 \quad (9)$$

$$\boldsymbol{n} \bullet k \nabla u = \bar{q}, \qquad \boldsymbol{x} \in \Gamma_2 \quad (10)$$

$$\boldsymbol{n} \bullet k \nabla u = h\left(u_{\mathrm{a}} - u \right), \qquad \boldsymbol{x} \in \Gamma_3 \quad (11)$$

where k and ρ represent the thermal conductivity and the density, Q is the heat source per unit mass. $\bar{u}(\boldsymbol{x})$ is the prescribed temperature, and $\bar{q}(\boldsymbol{x})$ is the prescribed heat flux. h denotes the convection heat-transfer coefficient, $u_{\mathrm{a}}(\boldsymbol{x})$ is the prescribed ambient temperature, and $\boldsymbol{n}$ represents the unit outward normal to the boundary.

If the field variable is approximated by the MLS scheme in Eq. (7), Eq. (8) and the boundary conditions Eqs. (9)-(11) cannot be satisfied exactly, which leads to residuals. Different ways to minimize the residuals correspond to different discretization schemes, such as the Galerkin method, the Petrov-Galerkin method, and the direct collocation method, all of which can be regarded as special cases of the weighted residual method[10]. In this paper, the residuals are minimized in a least-squares manner, as the sum of the squares of the residuals,

$$\Pi = \int_{\Omega} R^2(\boldsymbol{x}) \mathrm{d}\Omega + \int_{\Gamma_1} \alpha_1 \bar{R}_1^2(\boldsymbol{x}) \mathrm{d}\Gamma + \int_{\Gamma_2} \alpha_2 \bar{R}_2^2(\boldsymbol{x}) \mathrm{d}\Gamma + \int_{\Gamma_3} \alpha_3 \bar{R}_3^2(\boldsymbol{x}) \mathrm{d}\Gamma \quad (12)$$

which is to be minimized. $R(\boldsymbol{x})$ and $\bar{R}_i(\boldsymbol{x})$ refer to the residuals corresponding to the governing equation and the boundary conditions on Γ_i ($i = 1, 2, 3$) and α_i is the weight coefficient which is used as a penalty to enforce the boundary conditions. In Eq. (12), the function Π is an integral, which requires numerical quadrature in the final equations and increases the computational effort. To overcome this shortcoming, the following discrete functional is used instead.

$$\Pi = \sum_{K=1}^{m} R^2(\boldsymbol{x}_K) + \sum_{K=1}^{m_1} \alpha_1 \bar{R}_1^2(\boldsymbol{x}_K) + \sum_{K=1}^{m_2} \alpha_2 \bar{R}_2^2(\boldsymbol{x}_K) + \sum_{K=1}^{m_3} \alpha_3 \bar{R}_3^2(\boldsymbol{x}_K) \quad (13)$$

where m and m_i are the numbers of evaluation points in the domain and on the boundary Γ_i. The number of evaluation points is not necessarily equal to the number of nodes. According to the study on the stabilized form of partial differential equations by Onate et al.[11], including the residuals of the governing equations in the boundary conditions can increase the stability of the method. Thus, the governing equations in this method are satisfied not only on the evaluation points in the domain, but also on the boundaries. In this paper, all nodes were used as evaluation points in the first term of Eq. (13), with those on the boundaries as evaluation points in the other corresponding terms.

Let the variation of the function Π be equal to zero and invoke the arbitrariness of the variation $\delta \boldsymbol{u}$. The system equations are obtained as

$$\boldsymbol{K}\boldsymbol{u} = \boldsymbol{P} \quad (14)$$

where

$$K_{IJ} = \sum_{K=1}^{m} \left[k\nabla^2 N_I(\boldsymbol{x}_K) \right]\left[k\nabla^2 N_J(\boldsymbol{x}_K) \right] + \sum_{K=1}^{m_1} \alpha_1 N_I(\boldsymbol{x}_K) N_J(\boldsymbol{x}_K) + \sum_{K=1}^{m_2} \alpha_2 \left[\boldsymbol{n}\cdot k\nabla N_I(\boldsymbol{x}_K) \right]\left[\boldsymbol{n}\cdot k\nabla N_J(\boldsymbol{x}_K) \right] + \sum_{K=1}^{m_3} \alpha_3 \left[\boldsymbol{n}\cdot k\nabla N_I(\boldsymbol{x}_K) + hN_I(\boldsymbol{x}_K) \right] \bullet \left[\boldsymbol{n}\cdot k\nabla N_J(\boldsymbol{x}_K) + hN_J(\boldsymbol{x}_K) \right] \quad (15)$$

$$P_I = -\sum_{K=1}^{m} \left[k\nabla^2 N_I(\boldsymbol{x}_K) \right] \rho Q + \sum_{K=1}^{m_1} \alpha_1 N_I(\boldsymbol{x}_K) \bar{u} + \sum_{K=1}^{m_2} \alpha_2 \left[\boldsymbol{n}\cdot k\nabla N_I(\boldsymbol{x}_K) \right] \bar{q} + \sum_{K=1}^{m_3} \alpha_3 \left[\boldsymbol{n}\cdot k\nabla N_I(\boldsymbol{x}_K) + hN_I(\boldsymbol{x}_K) \right] hu_{\mathrm{a}} \quad (16)$$

The weight coefficients α_i have two functions: to enforce the boundary conditions and to balance the magnitudes of the residuals on the different boundaries. Thus, α_2 is set to a large number, 10^5 for example, and $\alpha_1 = \alpha_2 \left(k/L \right)^2$, and $\alpha_3 = \alpha_2 \left[\min\left(1, k/hL \right) \right]^2$, where L is the characteristic problem length.

Since the least-squares method is used to develop the discrete equations, and the weight coefficients are used to enforce the boundary conditions and balance the magnitudes of the residuals, the method is named the meshless weighted least-squares (MWLS) method.

3 Choice of Computational Parameters

The MWLS approximation requires some computational parameters, such as the order of the basis function and the dimension of the support domain. These parameters greatly influence the results.

Consider steady-state heat conduction in a bar of unit length and unit sectional area. The bar's side surfaces are adiabatic. So the problem is indeed 1-D. The temperature on the left end of the bar is fixed at 100℃ and the other end experiences a convection heat-transfer boundary whose ambient temperature is 0℃. The bar contains a distributed heat source $Q = 180x^2$ along the bar, where x refers to the distance from the left end. All the thermal physical parameters have unit values. The analytical solution for this problem is $u = -15x^4 - 12.5x + 100$. The MWLS method was used to solve this problem with 11 uniformly distributed nodes. Table 1 demonstrates the relative error for different orders of basis functions and different support radii. Here, "scale" in Table 1 means the ratio of the support radius to the nodal distance and the relative error is defined as

$$E_r = \sqrt{\sum_{I=1}^{n} \left(u_I^{\mathrm{num}} - u_I^{\mathrm{e}} \right)^2} \Bigg/ \sqrt{\sum_{I=1}^{n} \left(u_I^{\mathrm{e}} \right)^2} \quad (17)$$

where u_I^{num} and u_I^{e} represent the numerical and analytical solutions for node I.

Table 1 Relative error for different support radii and basis functions

Scale	Relative error (%)		
	Constant basis	Linear basis	Quadratic basis
2.25	21.8669	2.0435	0.4740
2.50	15.1452	0.2694	0.5978
2.75	11.1176	0.9572	0.6123
3.00	7.6668	1.6494	0.5740
3.25	3.9711	0.5003	0.2070
3.50	2.2156	1.2619	0.0692
3.75	1.2178	1.2533	0.2071
4.00	0.7748	0.7892	0.3398

Since the MWLS equation includes the second order derivatives, the quadratic basis function should give better results than linear or constant basis functions as the results in Table 1 indeed show. The relative error is the lowest when the support radius is 3.5 times the nodal distance for the quadratic basis function. The results in Table 1 show that the constant basis function with a larger support radius and the linear basis function also give acceptable results because the derivatives of the MLS shape function involve not only the derivatives of the basis functions, but also the derivatives of matrices $\boldsymbol{A}$ and $\boldsymbol{B}$, which are related to the weight function. Since the weight function, such as the cubic spline function, has higher order continuity, it is not surprising that basis functions of lower order can give reasonable results.

The MWLS method was also used to analyze the same problem but with a prescribed heat flux applied to the right end of the bar. Similar conclusions were drawn about the quadratic basis function with the support radius of 3.5 times the nodal distance as optimal. Thus, the following examples used these parameters.

4 2-D Numerical Examples

The following examples all analyze heat conduction in a rectangular domain as shown in Fig. 1. There is no heat source in the domain and the thermophysical parameters are set to unit values if not specified. All the EFGM computations used linear basis functions. Gauss quadrature (3×3) was used to evaluate the integrals, where the dimension of the background cell was consistent with the nodal distance.

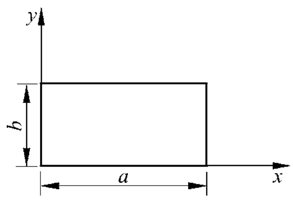

Fig. 1 Rectangular domain and coordinate system

4.1 Patch test

Consider a $1\,\mathrm{m}\times 1\,\mathrm{m}$ domain with a temperature distribution given by $u = x + y$. The boundary temperatures were set consistent with this distribution. Three nodal arrangements were used[12], one with regular spacing and two with irregular spacing, as shown in Fig. 2. The coordinates of Node 5 in irregular arrangement I are listed in Table 2, where six cases are analyzed. The nodal coordinates in irregular arrangement II are listed in Table 3. The numerical results show that the MWLS method exactly reproduces the distribution in all cases.

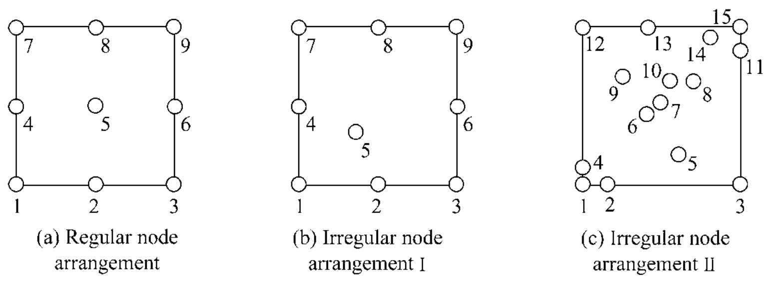

Fig. 2 Node arrangements

Table 2 Coordinates of Node 5 in irregular node arrangement I

	Case					
	1	2	3	4	5	6
x	0.55	0.05	0.05	0.95	0.45	0.15
y	0.55	0.05	0.40	0.90	0.45	0.15

Table 3 Coordinates for irregular node arrangement II

	Node						
	1	2	3	4	5	6	7
x	0.00	0.15	1.00	0.00	0.60	0.40	0.45
y	0.00	0.00	0.00	0.10	0.20	0.45	0.50

	Node							
	8	9	10	11	12	13	14	15
x	0.70	0.25	0.55	1.00	0.00	0.40	0.80	1.00
y	0.60	0.65	0.60	0.90	1.00	1.00	0.95	1.00

4.2 Heat conduction in a rectangular domain

Consider a rectangular domain in which $a = 1$ m and $b = 0.8$ m. The thermal conductivity is $k = 1.2\ \mathrm{W/(m{\cdot}℃)}$. A heat flux $\overline{q} = 500\ \mathrm{W/m^2}$ enters the domain from the upper boundary and the temperatures of the other boundaries are all fixed at $u_1 = 0℃$. The analytical solution is given by

$$u(x, y) = u_1 + \frac{4\overline{q}a}{k\pi^2}\sum_{m=0}^{\infty}\frac{\mathrm{sh}\dfrac{(2m+1)\pi}{a}y}{\mathrm{ch}\dfrac{(2m+1)\pi}{a}b}\,\frac{\sin\dfrac{(2m+1)\pi}{a}x}{(2m+1)^2} \tag{18}$$

Both the EFGM and the MWLS were used to solve the problem with a uniform 11×9 node distribution. The analytical EFGM and MWLS solutions are compared in Fig. 3, which shows that the three solutions coincide well. The MWLS results were more accurate than the EFGM results (1.21% versus 1.75%), but the MWLS method required only 18.4% of the computational time used by the EFGM.

4.3 Heat conduction in a square domain

Consider a square domain with side lengths of 200 m.

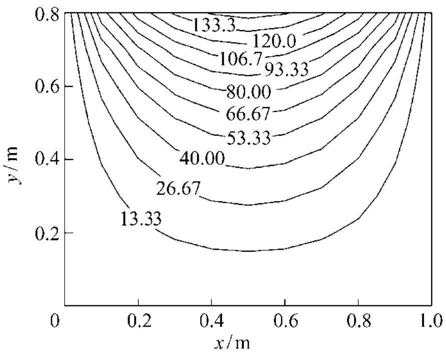

(a) Analytical solution

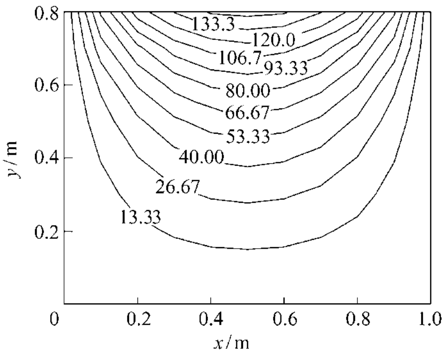

(b) EFGM solution

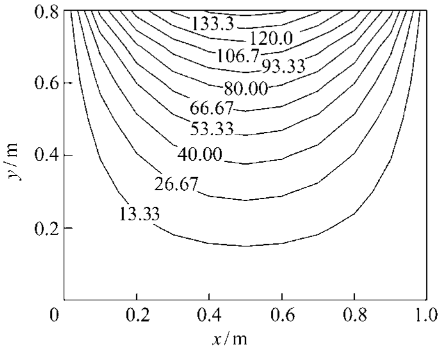

(c) MWLS solution

Fig. 3 Comparison of isotherms (℃)

Both the left and right edges are prescribed temperature boundaries whose temperature is 0℃, while both the top and the bottom edges receive a heat flux of $10\ \mathrm{W/m^2}$. Only one quarter of the domain needs be analyzed due to symmetry. The EFGM and MWLS methods were used for the analysis. Figure 4 compares the isotherms from the MWLS method and the EFGM results for an 11×11 node distribution. Figure 5 shows the temperature on the symmetry line $x = 100$ m, while Table 4 lists the CPU time for the two methods. The results obtained by these two numerical methods are very similar, while the MWLS solution time is less than one fifth that of the EFGM, mainly due to eliminating the numerical integration in favor of the discrete functional.

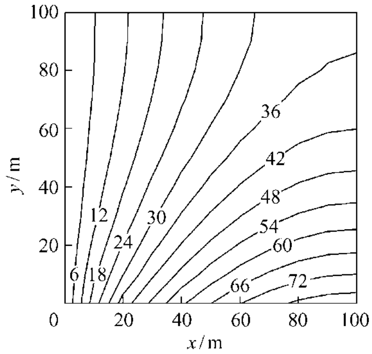

(a) EFGM solution

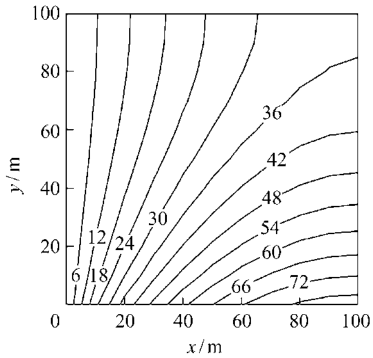

(b) MWLS solution

Fig. 4 Comparison of EFGM and MWLS isotherms (℃)

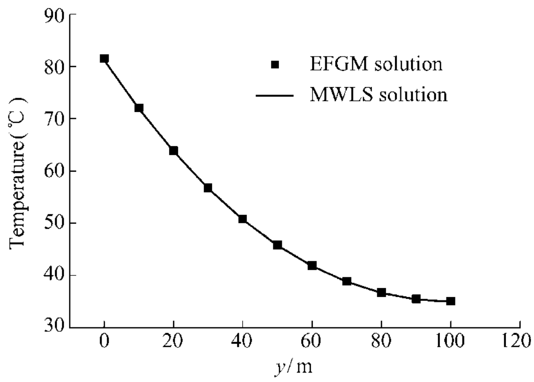

Fig. 5 Temperature distribution along the symmetry line

Table 4 Comparison of CPU time (s)

Method	Time for assembling process	Time for solving equations	Total solution time
MWLS	1.594	0.015	1.609
EFGM	9.036	0.015	9.051

5 Conclusions

The MWLS method, a meshless method based on least-squares discretization, was extended to solve steady-state heat conduction problems. The optimal computational parameters were determined by numerical tests. 2-D examples show that MWLS results coincide well with the analytical solution and that the MWLS method is more accurate than the EFGM.

Unlike Galerkin-type meshless methods, the MWLS method does not need numerical integration, which significantly improves the computational efficiency. When efficiency and accuracy are both taken into account, the MWLS method is an attractive meshless method. Further investigations of the MWLS method will consider transient heat conduction problems and heat convection problems.

References

[1] Lucy L B. A numerical approach to the testing of the fission hypothesis. *The Astron. J.*, 1977, **8**(12): 1013-1024.

[2] Gingold R A, Monaghan J J. Smoothed particle hydrodynamics: Theory and applications to non-spherical stars. *Mon. Not. Roy. Astron. Soc.*, 1977, **18**: 375-389.

[3] Monaghan J J. Smoothed particle hydrodynamics. *Annual Review Astronomics and Astrophysics*, 1992, **30**: 543-574.

[4] Belytschko T, Lu Y Y, Gu L. Element free Galerkin methods. *Int. J. Numer. Meth. Engrg.*, 1994, **37**: 229-256.

[5] Belytschko T, Krongauz Y, Organ D, et al. Meshless methods: An overview and recent developments. *Comput. Methods Appl. Mech. Engrg.*, 1996, **139**: 3-47.

[6] Li S F, Liu W K. Meshfree and particle methods and their applications. *Appl. Mech. Rev.*, 2002, **55**(1): 1-34.

[7] Zhang X, Liu Y. Meshless Methods. Beijing: Tsinghua University Press and Springer, 2004.

[8] Jiang B N. The Least-Square Finite Element Method: Theory and Applications in Computational Fluid Dynamics and Electromagnetics. Berlin: Springer-Verlag, 1998.

[9] Zhang X, Pan X F, Hu W, Lu M W. Meshless weighted least-square method. In: Proceedings of Fifth World Congress on Computational Mechanics. Vienna, Austria, July 7-12, 2002.

[10] Zhang X, Song K Z, Lu M W. Weighted residual method with compactly supported trial functions. *Acta Mechanica Sinica*, 2003, **35**(1): 43-49.

[11] Onate E, Perazzo F, Miquel J. A finite point method for elasticity problems. *Computers and Structures*, 2001, **79**: 2151-2163.

[12] Atluri S N, Zhu T. A new meshless local Petrov-Galerkin (MLPG) approach in computational mechanics. *Computational Mechanics*, 1998, **22**: 117-127.